Frontiers in Computing and Intelligent Systems
ISSN: 2832-6024 | Vol. 16, No. 2, 2026

Defect Detection of Can Cap Printing Based on Machine Vision

Yaqi Li *, Wei Hu

College of Electrical Engineering and Automation, Henan Polytechnic University, Jiaozuo, Henan, 454003, China
*** Corresponding author:** Yaqi Li

Abstract: To address the problems of high cost, low efficiency, and high rates of missed and incorrect detections in the production of metal can lid printing products, an online inspection system for metal can lids was designed based on machine vision. Firstly, threshold segmentation was performed using the maximum inter-class variance method, and the detection area of the can lid was extracted through feature extraction and intersection operations. For surface printing detection, a printing defect detection method based on constructing a difference model was proposed. The Sobel operator was used to extract the edge information of the image to create a difference model, and template matching and the detection area were used to process the tested image using similarity measurement, affine transformation, and scaling of gray values, etc. Finally, the obtained images were input into the difference model for the final defect detection. Experiments were conducted by detecting a large number of tested images with different defects to verify the effectiveness of the scheme.

Keywords: Metal Can Lid; Printing Inspection; Template Matching; Difference Model.

1. Introduction

During the production process of industrial metal can lid printing products, the printing equipment may suffer from component wear or aging due to long-term high-speed operation. Additionally, unstable factors in the production environment and transportation process can easily lead to product quality issues such as surface scratches, missing prints, omissions, ink spots, et al[1-2]. These defects not only significantly reduce the printing efficiency but also cause economic losses to the manufacturers. Traditional metal can inspections are mostly carried out manually[3], using the visual method. Although this method can detect some defective products, it has disadvantages such as high cost, false detection, missed detection, and low measurement efficiency and accuracy. Therefore, new detection methods are needed to solve these problems. With the development of technology, machine vision image processing technology has been widely applied in the quality inspection of printing products.

Chen Kaixuan[4] et al. processed the obtained image using the Sobel operator and then analyzed it through mathematical morphology methods, eliminating the contour artifacts caused by the double reflection effect of paper and mechanical vibration, and improving the detection accuracy; Wang Gang[5] et al. solved the problem that template matching is easily affected by external interference by improving the method of determining the similarity measurement between matches by replacing the Euclidean distance with the Manhattan distance, greatly improving the stability of the algorithm; Ding Xiaoling[6] et al. targeted items with less texture, screened the gradient features through the DOT algorithm to improve the detection accuracy and robustness of template matching; Chen Wanjun[7] et al. proposed a printing image defect detection method based on interest point feature matching, first extracting the image feature points, then completing the matching of the feature points of the two images through the nearest neighbor interpolation method[8-9], and then using the least squares optimization algorithm to calculate the transformation matrix to achieve defect detection. This method has a high requirement for the accuracy of feature point extraction, and must also comply with the defect detection criteria specified by the manufacturer. Zhu Yili[10] et al. proposed an improved Canny edge algorithm based on genetic ant colony algorithm, although it can effectively improve the efficiency of extracting image edge information, due to the slow convergence speed of the genetic ant colony algorithm itself. Based on deep learning algorithms usually require a large number of samples to train the model, and during the training process, a certain computing capacity is required. Especially when the image size is large or the model structure is complex, the time required for model training and detection is often long, and the training and detection of the model consume a lot of time, which is difficult to meet real-time requirements.

This paper takes metal printed can lids as the research object. Through the methods of threshold segmentation and feature extraction, the metal can lid area is segmented and extracted. For surface printing detection, a template matching method based on extracting shape and gray value information from the template image to construct a difference model is used to extract the defect area, achieving visual detection of the printed parts of the metal can lids. This algorithm has the characteristics of simple structure and low computational requirements, and can adapt to the operation speed requirements of the production site, ensuring the real-time and effectiveness of the detection.

2. Overall design of the printing defect detection system

(1) Detection Objectives and Demand Analysis

This paper focuses on the study of metal printed can lids. In daily life, such printed surfaces often have various types of defects such as missed printing, over-printing, scratches, and ink spots [11], as shown in Figure 1.

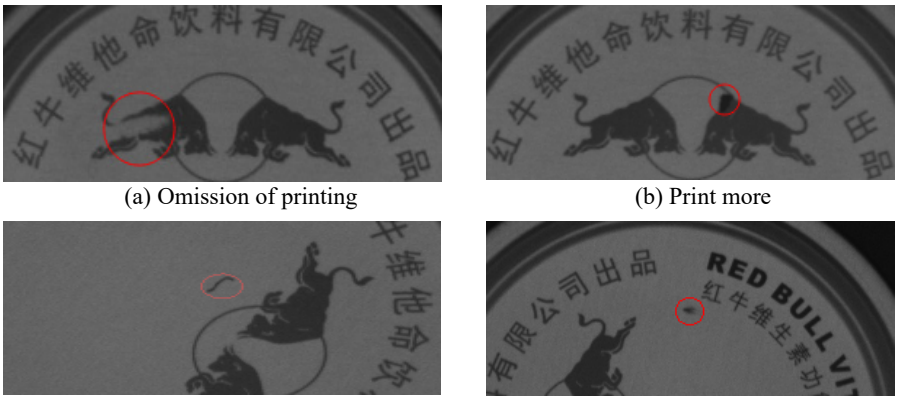

(a) Omission of printing (b) Print more

(c) Scratch (d) Dots of ink

Figure 1. Common Defect Types

Based on the actual production site requirements, the quality standards for the metal tank cover printing defect detection of this system are as follows: the detection accuracy should be no less than 0.5mm×0.5mm, the detection speed should be able to adapt to the production line speed of 90-120m/min, and the detection area should be 150mm×150mm.

(2) Image Acquisition Device

Based on the actual conditions such as the size of the tank cover and the requirements for detection accuracy, the selection of hardware equipment was carried out. Among them, an industrial camera of the acA1300-60 gm type from the German company Basler was chosen. It uses a GigE interface and supports gigabit network transmission. It is combined with an industrial lens of the M1214-MP2 type produced by the company Computar as the image acquisition device. Considering that the surface material of the metal printed products has reflective properties, the light source part chose an LED dome light source. By means of diffuse reflection, the light is evenly irradiated onto the surface of the detected object, which can effectively reduce mirror reflection and facilitate the acquisition of the printed image of the metal tank cover.

(3) Printing Defect Detection Process

The defect detection algorithm based on the difference model can be divided into two parts: the template creation of the difference model and the matching and comparison based on the difference model. Firstly, an image without printed defects is selected as the standard image template. Threshold segmentation, segmentation of connected domains, feature selection, etc. are carried out to obtain the detection area. Then, edge detection is performed on the template image and edge information is extracted. The difference model threshold is set according to actual needs, and the difference model is established based on the edge information and the threshold. Finally, the detection area extraction and registration operations are performed on the tested image, and the defect of the image is judged and detected based on the difference model. The overall process is shown in Figure 2.

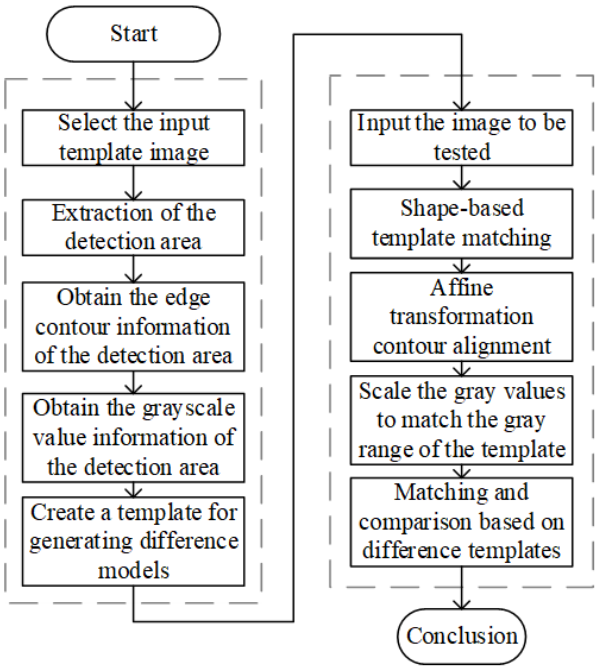

Figure 2. Workflow for Printing Defect Detection Based on Difference Model

3. Printing Defect Detection Based on Difference Model

(1) Extraction of the Detection Area

Using the established image acquisition device, the metal tank cover was captured for image collection. The original image of the printed tank cover obtained is shown in Figure 3.

Figure 3. Original image of the tank cover printing

As shown in Figure 3, there is a significant difference in the gray values between the lid area and the background area. The extraction of the detection area can be achieved by using the maximum inter-class variance method[12] for threshold segmentation of the image. Assuming the image is , the segmentation thresholds for the foreground and background are, and the image size is Initialize the threshold and calculate the ratio of the pixel points of the foreground and background to the total pixel points of the image as and:

$$\omega_1 = N_1 / M * N \tag{1}$$

$$\omega_2 = N_2 / M * N \tag{2}$$

The overall average gray level of the entire image is β, while the average gray levels of the foreground and background are β_1 and β_2 respectively:

$$\beta = \omega_1 * \beta_1 + \omega_2 * \beta_2 \tag{3}$$

Inter-class variance σ:

$$\sigma = \omega_1 \omega_2 (\beta_1 - \beta_2)^2 \tag{4}$$

The threshold that maximizes the inter-class variance is determined by using a traversal search method. When the inter-class variance reaches its maximum, the difference between the foreground and the background is the most significant. The threshold obtained at this point is the optimal segmentation threshold, and the segmentation effect is shown in Figure 4.

Figure 4. Threshold Segmentation Map for Tank Cover Printing

The threshold segmentation is applied to obtain the image, which is then processed by the connected component analysis[13]. The regions that are not connected to each other are divided into different areas, and each area is distinguished by a different color. The result is shown in Figure 5.

Figure 5. Segmentation Map of Printed Connected Domains on Tank Cover

By observing the image after the segmentation of connected components, it can be seen that the area on the left is non-image information. Therefore, the area features of the remaining independent connected components are screened. The regions with pixel areas smaller than a certain threshold are filtered out to achieve the effect of retaining only the main image information and eliminating the influence of noise. The effect after screening is shown in Figure 6.

Figure 6. Area Filtering Diagram

Finally, the minimum enclosing rectangle and the minimum enclosing circle of the remaining main image information are drawn as the main body, and the intersection of the two is calculated, which is the segmented detection area. The segmented effect is shown in Figure 7.

Figure 7. The detection area extracted from

(2) Template Creation for Difference Models

The creation of the difference model requires extracting the edge contour information from the detection area. Firstly, a shape template is created, and a scalable and deformable shape model is established as shown in Figure 8.

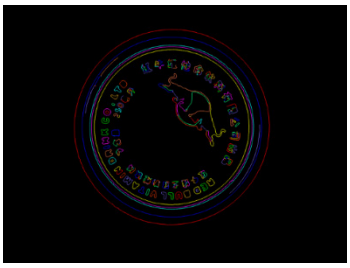

Figure 8. Scalable Shape Model

When observing the scalable shape model, the contour edge information is lost. To create a difference model with complete edge information, in this paper, the Sobel edge algorithm is used to extract the contour edge information from the template image[14]. Two convolution factors, A and B, are used as edge detection filters to perform convolution processing on each pixel in the image. Both A and B convolution factors are third-order matrices. The two convolution factors are used to perform convolution on each pixel in the template image, and are the gray value results obtained after convolution in the horizontal and vertical directions respectively. According to Equation(5), the

convolution results in the horizontal and vertical directions are calculated to obtain the gray value G of this pixel point:

$$G = \sqrt{G_x^2 + G_y^2} \tag{5}$$

After convolving the template image with the Sobel operator, the noise was smoothed, and precise image edge information was provided. This enabled the complete edge information necessary for the creation of the difference model, and the effect is shown in Figure 9.

Figure 9. Scalable Shape Model

The core of the difference model lies in extracting shape and grayscale value features from the template image. Previously, edge shape information was extracted, and it is necessary to further correlate the grayscale information of the image to enhance the robustness of the detection algorithm against minor grayscale fluctuations. To this end, two parameters, absolute threshold and relative threshold , are introduced. The absolute threshold represents the maximum allowable absolute grayscale difference between the image to be detected and the template image; the relative threshold represents the maximum allowable relative grayscale difference between the image to be detected and the difference image. Based on these two thresholds, the maximum grayscale value image and the minimum grayscale value image can be calculated.

Let the template image be $i(x, y)$, and the difference image be $v(x, y)$. The absolute threshold and relative threshold are a, b , and these two thresholds need to be manually set according to the actual detection conditions. The calculation formulas for the maximum gray value image $t_u(x, y)$ and the minimum gray value image $t_l(x, y)$ are as follows:

$$t_u(x, y) = i(x, y) + \max\{a_u, b_u v(x, y)\} \tag{6}$$

$$t_l(x, y) = i(x, y) - \max\{a_l, b_l v(x, y)\} \tag{7}$$

By determining two thresholds, the image with the maximum gray value limit in the detection area and the image with the minimum gray value limit can be obtained and stored in the template. The effects are respectively shown in Figures 10 and 11, which are used for comparison and matching with the target image in the subsequent matching and comparison experiments.

Figure 10. Image with Maximum Gray Value

Figure 11. Image with the Minimum Gray Value

In summary, the core idea of establishing the difference model is to extract the edge information of the template image, and then combine it with the original template image as the input of the difference model. The maximum gray value map and the minimum gray value map are calculated, and the results are finally stored in the difference model for subsequent experiments for comparison.

(3) Matching Comparison Based on the Difference Model

The matching comparison based on difference modeling can be divided into two steps: Firstly, according to the template matching principles and registration of the standard graphic model, the image to be detected is aligned and its grayscale is scaled based on the standard graphic template; then, the grayscale of the detected image and the grayscale of the difference model are compared, and the defect areas existing in the detected image are determined and selected according to the actual accuracy requirements.

Apply the Sobel operator to both the ideal image and the image to be detected for edge detection, and calculate the direction vectors. Then, search and match the shape contours based on the similarity measure that is not affected by occlusion and disorder.

The set of pixel points of the template image is $P_i = (r_i, c_i)^{\mathrm{T}}$, the set of corresponding point's associated direction vectors is $d_i = (t_i, u_i)^{\mathrm{T}}, i = 1, 2, ..., n$, and the corresponding points in the image to be tested are $q(r, c)$. The corresponding associated direction vectors $e_{\mathrm{r,c}} = (V_{\mathrm{r,c}}, W_{\mathrm{r,c}})^{\mathrm{T}}$, $P_i^{'}$ and $d_i^{'}$ are the pixel point sets and corresponding gradient vectors of the model after affine transformation. Based on the inner product of the gradient vectors of the points in the template image and the corresponding points in the image to be tested, the similarity measure s that avoids confusion and interference from foreign objects is obtained as follows:

$$\begin{aligned} s &= \frac{1}{n}\sum_{i=1}^{n}\frac{d_i^{\pi} e_{q+p'}}{d_i^{\pi} \times e_{q+p'}} \\ &= \frac{1}{n}\sum_{i=1}^{n}\frac{t_i^{'} V_{r+r_i^{'},c+c_i^{'}} + u_i^{'} W_{r+r_i^{'},c+c_i^{'}}}{\sqrt{t_i^{'2} + u_i^{'2}}\sqrt{V_{r+r_i^{'},c+c_i^{'}}^2 + W_{r+r_i^{'},c+c_i^{'}}^2}} \end{aligned} \tag{8}$$

By adjusting the matching parameters using the least squares method, a sub-pixel accuracy level of pose that is more precise than the search space is achieved. This also reduces the computational load of the pyramid search strategy for matching, ultimately achieving the goal of accurately and quickly locating the image to be detected.

After the positioning of the image to be tested is completed, since there may be spatial position and angle differences between the template image and the image to be tested, a rigid

affine transformation[15] needs to be performed using the homogeneous rotation matrix $HomMat2D$ to complete the position correction. The rotation matrix R and the translation vector T are the two important components of the homogeneous rotation matrix $HomMat2D$, and their formulas are:

$$\begin{aligned} HomMat2D &= \begin{pmatrix} R & T \\ 0 & 1 \end{pmatrix} \\ &= \begin{pmatrix} 1 & 0 & T \\ 0 & 1 & \\ 0 & 0 & 1 \end{pmatrix} \cdot \begin{pmatrix} R & & 0 \\ & & 0 \\ 0 & 0 & 1 \end{pmatrix} \\ &= H(T) \cdot H(R) \end{aligned} \tag{9}$$

$$R = \begin{pmatrix} \cos(phi) & -\sin(phi) \\ \sin(phi) & \cos(phi) \end{pmatrix}, T = (T_x, T_y) \tag{10}$$

Among them, R represents the rotation matrix, phi is the angle difference between the test image and the template image, and the rotation angle is added to the homogeneous rotation matrix to correct the angle deviation between the test image and the template image. T is the translation vector, and T_x and T_y are the translation distances along the axes x and y respectively. The translation is added to the homogeneous rotation matrix to position the test image and the template image in the same location, eliminating the distance deviation between the test image and the template image, thereby making the test image and the template image overlap.

Since algorithms such as affine transformation will change the gray values of the image to be inspected, in order to compare the gray value information of the image to be inspected with that of the difference model, it is necessary to align the gray value ranges of the two. Taking the gray value range of the difference model as the reference, the gray value range of the image to be inspected should be scaled to compensate for the effects caused by algorithms such as affine transformation[16].

Firstly, the maximum inter-class variance method is used to perform threshold segmentation on the standard template image and the image to be tested, respectively, to obtain the foreground and background regions of the two images. Then, the gray average value M of the regions is obtained using formula (11):

$$M = \frac{\sum_{p \in ROI} g(p)}{F} \tag{11}$$

In Equation (11), ROI represents the region of interest, . F . denotes the area of the region, p indicates the pixels of the region, and $g(p)$ represents the gray value of that point.

The average gray values of the foreground and background of the template image, the average gray values of the foreground and background of the test image after registration, and the average gray value of the background of the test image after registration are respectively M_{fore}, M_{back}, M'_{fore} and M'_{back}.

Then, using formulas (12) and (13), the proportion factor M_t and the offset A_1 are calculated respectively:

$$M_t = \frac{M_{\text{fore}} - M_{\text{back}}}{M'_{\text{fore}} - M'_{\text{back}}} \tag{12}$$

$$A_1 = M_{\text{fore}} - M_t \times M'_{\text{fore}} \tag{13}$$

The difference model is used as the benchmark to map the grayscale values of the input image to be detected. That is, the scaling processing of the grayscale value range is carried out. After scaling, the grayscale value of the corresponding pixel point is g', and the calculation formula is:

$$g' = M_t \times g + A_1 \tag{14}$$

After the above processing, the gray value range of the image to be detected is completely aligned with the gray value range of the difference model. Within the same gray value range, the current input image $c(x, y)$ to be detected is compared with the image $t(x, y)$ of the difference model:

$$c(x, y) > t_u(x, y) \vee c(x, y) < t_l(x, y) \tag{15}$$

The total area of all regions corresponding to images with a gray level lower than the minimum gray level in the difference model and the regions corresponding to images with a gray level higher than the maximum gray level in the difference model is output. The output part represents the regions with abnormal gray values, that is, the regions where defect features have been detected, and through the selection of area features, the purpose of controlling the detection accuracy is achieved.

4. Experimental Results and Analysis

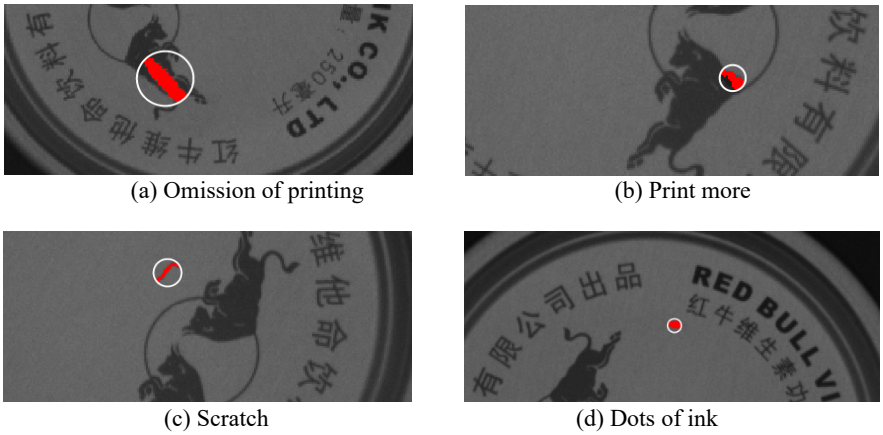

(a) Omission of printing (b) Print more

(c) Scratch (d) Dots of ink

Figure 12. Detection effect

In order to verify the effectiveness of the algorithm, artificial defect samples were generated based on the actual defect characteristics of the on-site products. The batch printed image containing the defect samples was input into the system for the defect detection experiment. Some of the detection results are shown in Figure 12.

The experimental results show that the algorithm performs well in recognition, and all the indicators meet the detection requirements. The total number of images collected in the experiment was 1000, among which normal printed image samples accounted for approximately 1/5. In the defect samples, some metal can lids had multiple defects. Calculated by the number of defects, the sample set contained a total of 1032 defects. When the input sample was a defect sample and the recognition result was also a defect sample, it was counted as a successful recognition of the defect sample. The algorithm successfully identified 801 samples with defects in total, with a missed detection rate of 0.86%; among the 1032 defects, 981 were correctly identified, with an accuracy rate of approximately 95.06%; the number of misjudged normal samples was 1, and the false detection rate was approximately 0.52%.

Apart from the accuracy rate of detection, the algorithm's computing speed and the number of defect types it can identify are also important indicators for evaluating the superiority of the algorithm. Defect detection is generally carried out in the horizontal operation section of the production process. The algorithm's computing speed needs to be able to match the operating speed requirements of the production line; the number of defect types that can be identified is mainly used to measure the practicality and universality of the algorithm. In actual production, due to the influence of the environment and materials, the defects on the surfaces of different printed products vary greatly. The algorithm has the ability to identify more defect types, covering the common defect types in the industry, which means it has higher application value in actual production. In the experiment, the time consumed for each image recognition detection was recorded and the average value was calculated to obtain an average running time of approximately 55.67ms, which can meet the real-time requirements of production.

In order to further verify the effectiveness of the defect detection method proposed in this study, several detection methods proposed in literatures [17] to [20] were selected for algorithm reproduction and comparison experiments. To ensure the consistency of the comparison experiments, all processing steps not explicitly described in the literature were uniformly handled according to the corresponding steps in this study. Based on the data set constructed above, the evaluation indicators such as accuracy rate, missed detection rate, false detection rate and detection speed were statistically analyzed. The experimental results are shown in Table 1

Table 1. Comparison Results of Algorithm

Method	Accuracy (%)	Missed Detection Rate (%)	False detection rate (%)	Detection speed (ms)
Reference [17]	87.23	17.45	1.42	352
Reference [18]	83.56	13.23	1.56	895
Reference [19]	88.12	15.71	2.49	320
Reference [20]	81.35	19.56	8.63	1549
The algorithm in this article	95.06	0.86	0.52	56

5. Conclusion

Currently, the methods based on deep learning for printing defect detection are generally highly dependent on the size of the data set, and the model training process requires high computing power. As the complexity of the model increases, the training time also increases. Considering that it is difficult to obtain large-scale defect samples from the production site for the research object, and the existing methods based on classical pattern recognition generally have room for improvement in terms of detection real-time performance and accuracy, this study is based on machine vision technology and focuses on the automatic threshold segmentation and edge information extraction of the collected images for the extraction of detection areas. A defect detection scheme based on template matching using a difference model is proposed and applied to the defect detection in the printing production of metal tank covers. The experimental results show that this scheme can effectively detect different types of defects in production, achieving an accuracy rate of 95.06%, with a detection speed of 56ms. It has good detection speed and recognition rate, with a false detection rate and missed detection rate of 0.52% and 0.86% respectively, both of which are low, and can replace the current manual detection adopted by enterprises, meeting the actual production site requirements in terms of detection real-time performance and effectiveness.

References

[1] Zhao Fan, Li Yinhua, Wang Bo. Design of an Online Inspection System for Water-Slave Paper [J]. Packaging Engineering,2018,39(09):165-170.

[2] Jiang Qianbiao. Research on Online Detection System for Industrial Product Defects [D]. Zhejiang University of Technology, 2017

[3] Meng Chao. A New Chapter in Packaging Printing Inspection: Machine Vision [J]. Printing Magazine, 2017(08): 59-61.

[4] CHEN Kai-xuan, LIU Xin. A Method for Eliminating Shadow of Contour in Printing Defect Detection[J].Joumal of Xian University of Technology, 2017, 33(4): 486-491.

[5] WANG Gang, SUN Xiao-liang, SHANG Yang, et al. A Robust Template Matching Algorithm Based on Best-Buddies Similarity[J]. Acta Optica Sinica, 2017,37(3):274-280.

[6] DING Xiao-ling, ZHAO Qiang, LI Yi-bin, et al. Mod-ified Target Recognition Algorithm Based on Template Matching[J]. Journal of Shandong University (Engi-neering Science), 2018, 48(2): 1-7.

[7] Chen Wanjun, Chen Yajun, He Yi. Detection of Printing Image Defects Based on Feature Matching of Interest Points [J]. Packaging Engineering, 2007, 28(3): 22-23.

[8] Liu Zhijun, Cai Chao, Peng Xiaoming. A Novel Regularized Image Interpolation Method Based on Genetic Algorithm [J]. Journal of Image and Graphics, 2018, 9(8): 934-940.

[9] Cheng Huifang. Research on Image Rotation Algorithm Based on Radial Basis Function [D]. Lanzhou University, 2016.

[10] ZHU Hui-li, YANG Yong-zeng. Improved CANNY Edge Algorithm Based on Genetic and Ant Colony Algorithm [J]. Digital Printing, 2019, (1): 46-51.

[11] CHEN Ya-jun, ZHANG Er-hu. Research On-Line De-fect Detection System for Printed-Matter Based on Image Processing[J]. Packaging Engineering, 2005,26(6):64-66.

[12] YANG Shan-tang, DAO Hua-xia, GUI Yang-zhang, etal. The Detection Method of Lane Line Based on the Improved Otsu Threshold Segmentation[J]. Applied Mechanics and Materials, 2015, 3844: 354-358

[13] BI Sheng, XUE Jiong, WANG Yu. Building Image Segmentation Based on Visual Saliency and Connected Domain Segmentation [J]. Application Research of Computers, 2020, 37(S2): 359-361.

[14] RANA H, NEERU N. A Comprehensive Review of Sobel Edge Detector Using Gray Scale Images[J]. Re-search Cell: An International Journal of Engineering Sciences, 2016, 22: 688-692.

[15] ZENG Wen-feng, LI Shu-shan, WANG Jiang-an. Translation Rotation and Scaling Changes in Image Registration Based Affine Transformation Model [J]. Infrared and Laser Engineering, 2001, 30(1): 18-20, 17.

[16] MA Qian-ru, YE Ji-min. Convergence and Consistency Analysis of FastICA Algorithm[J]. Computer Engi-neering and Applications, 2020, 56(2): 35-41.

[17] FU Xing-yong, REN De-jun, YAN Zha-jie, et al. Trans parent Box Defect Detection Based on Template Matching [J]. Software Guide, 2019, 18(3): 187-190.

[18] ZHAO Xiang-yu, ZHOU Ya-tong, HE Feng, et al. Printing Defects Detection Based on Template Matching under Disturbing Industrial Environment [J]Packaging Engineering, 2017, 38(11): 187-192.

[19] SUN Lian-jie, FAN Zhen. Target Detection of Fiber Transceiver Board PCB Based on Template Matching[J]. Computer Applications and Software, 2018, 35(1):128-131,190.

[20] HAN Bin, LIU Yi-an, WANG Shi-tong. Image Processing-Based Defect Inspection of Printed Material[J]. Automation Technique and Application, 2002, (3):37-38.